

The Influence of Eastern Pacific Tropical Cyclone Remnants on the Southwestern United States

ELIZABETH A. RITCHIE AND KIMBERLY M. WOOD

Department of Atmospheric Sciences, The University of Arizona, Tucson, Arizona

DAVID S. GUTZLER

Department of Earth and Planetary Sciences, University of New Mexico, Albuquerque, New Mexico

SARAH R. WHITE

Department of Atmospheric Sciences, The University of Arizona, Tucson, Arizona

(Manuscript received 17 February 2010, in final form 16 June 2010)

ABSTRACT

Forty-three eastern North Pacific tropical cyclone remnants with varying impact on the southwestern United States during the period 1992–2005 are investigated. Of these, 35 remnants (81%) brought precipitation to some part of the southwestern United States and the remaining 8 remnants (19%) had precipitation that was almost entirely restricted to Mexico, although cloud cover did advect over the southwestern United States in some of these cases. Although the tropical cyclone–strength winds rapidly diminish upon making landfall, these systems still carry a large quantity of tropical moisture and, upon interaction with mountainous topography, are found to drop up to 30% of the local annual precipitation.

Based on common rainfall patterns and large-scale circulation features, the tropical cyclones are grouped into five categories. These include a northern recurving pattern that is more likely to bring rainfall to the southwestern United States; a southern recurving pattern that brings rainfall across northern Mexico and the Gulf Coast region; a largely north and/or northwestward movement pattern that brings rainfall to the west coast of the United States; a group that is blocked from the southwest by a ridge, which limits rainfall to Mexico; and a small group of cases that are not clearly any of the previous four types. Composites of the first four groups are shown and forecasting strategies for each are described.

1. Introduction

The southwestern United States has a mild, arid or semiarid, continental climate characterized by low annual precipitation, abundant sunshine, low relative humidity, and relatively large annual and diurnal temperature ranges. The regional topography consists mainly of high plateaus, with numerous mountain ranges, canyons, valleys, and normally dry arroyos. Elevation ranges from sea level to well over 3000 m above sea level. Arizona, Colorado, and New Mexico receive about 50% of their annual rainfall from July to September and are strongly impacted by summertime weather systems from the tropics and

subtropics associated with the North American monsoon (NAM).

Summertime rains in the NAM-impacted states fall almost entirely during brief, but frequently intense, thunderstorms. It is common for over 90% of summer rain to fall in less than 5 days.¹ In general, a southeasterly circulation from the Gulf of Mexico brings moisture into the region (Adams and Comrie 1997; Douglas et al. 1993; Higgins et al. 1997; Higgins et al. 1999). Strong surface heating combined with orographic lifting as the air moves over higher terrain produces the thunderstorms. The position of the Gulf of Mexico high pressure system is critically important for determining the location of the monsoonal moisture and summer precipitation in the

Corresponding author address: E. A. Ritchie, Dept. of Atmospheric Sciences, The University of Arizona, 1118 E 4th St., Rm. 254, Tucson, AZ 85721-0081.
E-mail: ritchie@atmo.arizona.edu

¹ Numbers are validated from the rainfall records archived at the National Climatic Data Center (NCDC).

North American southwest (Higgins et al. 1997). July, August, and September are the rainiest months over most of the region, producing, on average, approximately 40%² of the annual rainfall (Douglas et al. 1993). However, relatively small zonal differences in the location of the high pressure system over the Gulf of Mexico can regionalize seasonal rainfall anomalies (Comrie and Glenn 1998; Gutzler 2004). An example is 1994 when Tucson, Arizona, received 29% (8.5 cm) of its annual rainfall during the monsoon season while Albuquerque, New Mexico, received 57% (16.1 cm).

Apart from moisture transport from the Gulf of Mexico, other sources of moisture contributing to precipitation during the NAM include northward-propagating surges of low-level, moist, cooler air up the Gulf of California (Stensrud et al. 1997; Fuller and Stensrud 2000; Higgins et al. 2004) and inverted troughs (Douglas and Englehart 2007; Bieda et al. 2009). Gulf of California moisture surges, more commonly known as gulf surges, can be triggered by the passage of tropical easterly waves. The intensity and impacts of easterly wave-induced surges vary based on the timing of the easterly wave and the timing, presence, or absence of a midlatitude trough passing over the western United States (Stensrud et al. 1997). These gulf surges can also be initiated by a tropical cyclone passing the Gulf of California (Douglas and Leal 2003; Higgins and Shi 2005). In the NAM region, inverted troughs, or subtropical upper-level lows, which propagate westward along the southern periphery of the subtropical ridge (Finch and Johnson 2010) can influence upper-level dynamics and thus are important in enhancing convective precipitation (Douglas and Englehart 2007; Bieda et al. 2009). Changes in the frequency of inverted troughs within a single season can greatly impact overall summertime rainfall amounts in a given year (Douglas and Englehart 2007).

Variability associated with the NAM influences the impacts of each of these mechanisms from year to year and within the same season (e.g., Higgins et al. 1999; Englehart and Douglas 2006; Douglas and Englehart 2007). When the frequency, intensity, and/or precipitation resulting from these sources decreases, other, less regular moisture sources have the potential to contribute significant portions of summer rainfall during the NAM. One of these additional sources of tropical moisture is occasionally advected into the North American arid southwest region from the eastern North Pacific and the Gulf of Mexico in the form of tropical cyclone remnants. Although less well studied, the remnants of

tropical storms can advect over the southwestern United States if synoptic conditions are favorable (e.g., Collins and Mason 2000; Ritchie et al. 2006; Corbosiero et al. 2009).

Tropical cyclones strongly affect precipitation totals along the coast of Mexico (Reyes and Mejía-Trejo 1991; Englehart and Douglas 2001; Jáuregui 2003; Larson et al. 2005). Although the tropical cyclone-strength winds typically diminish rapidly upon making landfall, these systems still contain a large quantity of tropical moisture and, upon interaction with mountainous terrain, have the potential to drop copious amounts of precipitation in localized areas. These precipitation events are responsible for many of the largest floods on record in small canyons across the southwestern United States and, therefore, have important effects on land use and landscape evolution (Etheredge et al. 2004). Furthermore, these systems are traditionally difficult to forecast accurately due to the nature of their interaction with the midlatitude flow (e.g., Gutzler et al. 2005; Gutzler et al. 2009).

To better understand the impacts that changing climate may have on water resources in the arid southwestern United States, it is necessary to first understand the role that heavy precipitation events such as tropical cyclone remnants play in our current climate. This study presents an analysis of the common synoptic circulations associated with characteristic tropical cyclone remnant tracks across the southwestern United States. Our study differs considerably from a recent study by Corbosiero et al. (2009) in the following ways. First, they investigated only tropical cyclones that moved north of 25°N while still at tropical storm strength ($>17 \text{ m s}^{-1}$ maximum surface winds). Their group of tropical cyclones comprises only 20% of the total tropical cyclone remnants that impact the southwestern United States. Second, they discuss a single, all-encompassing composite synoptic pattern made up of a 20-yr subset of all their cases. We define and discuss individual composite categories, in terms of their rainfall swaths and synoptic circulations patterns. Many of the remnants in our database, which do not meet the latitudinal criteria set by Corbosiero et al. (2009), have considerable rainfall impacts throughout the southwestern United States, both negative and positive, even though the associated surface winds may be relatively weak. They are a challenge to forecast because small differences in the advection of these systems can turn a potential rain maker into a cloud-cover, no-rain event. Thus, it behooves us to attempt to better understand these systems as a first step toward providing forecaster guidance. In contrast to Corbosiero et al. (2009), we present and discuss composite large-scale patterns and rainfall swaths associated with each of four main categories of tropical cyclone remnants,

² Value calculated for statewide averages over AZ, CO, and NM supplied by the Western Regional Climate Center.

which produce distinctly different rainfall swath patterns and regional impacts from each other.

In this study we will investigate the impacts that tropical cyclone remnants from the eastern North Pacific have on precipitation in the southwestern U.S. region. We will study their climatological impacts, the nature of the large-scale circulations that advect them across the southwestern United States, and their associated rainfall patterns. The data and methodology used in this study will be described in section 2, some climatological results will be presented in section 3, a description of the composite large-scale patterns associated with tropical cyclone remnants in the southwestern United States and their associated rainfall patterns will be presented in section 4, and a summary and conclusions will be provided in section 5.

2. Data and methodology

We wish to consider the impacts of all eastern North Pacific tropical cyclone (TC) remnants on the United States, and therefore the region that is considered in this study is somewhat larger than the traditional “southwest” United States. The region of study includes the U.S. states of California, Nevada, Utah, Colorado, Arizona, New Mexico, and Texas (outlined in Fig. 3a) as well as Mexico.

A tropical cyclone remnant is defined for the purposes of this study as being either a complete tropical cyclone or a cohesive moisture segment that separated from the parent low-level circulation due to increased upper-level environmental flow that moved within 550 km of the west coast of Mexico or the United States. This definition differs considerably from that of Corbosiero et al. (2009), who considered only complete tropical cyclones that moved north of 25°N while still at tropical storm or greater strength. Their dataset comprises only 20% of the total tropical cyclone remnants that impact the region.

Near-coastal tropical cyclone remnants from 1992 to 2005 were identified using the National Hurricane Center (NHC) best-track data, in association with Geostationary Operational Environmental Satellite (GOES) infrared (IR) and water vapor (WV) imagery, which are freely available from the Global International Satellite Cloud Climatology Project (ISCCP) B1 Browse System (GIBBS; imagery available online at <http://www.ncdc.noaa.gov/gibbs/>). First, the NHC database was used to obtain the 6-h latitude and longitude positions for each eastern North Pacific cyclone between 1992 and 2005. A subset of these tropical cyclones was then chosen as having potential impacts on Mexico and the southwestern United States if their remnants approached within 550 km of the Mexico or

U.S. coastlines, following the methodology of Englehart and Douglas (2001). All candidate remnants were tracked every 3 h until they were no longer identifiable in satellite imagery. For all cases, the areal extent of the tropical cyclone remnant moisture field at each time step was determined from IR and WV imagery and used to extract the remnant-associated precipitation.

The unified U.S.–Mexico daily gridded precipitation analyses acquired from the National Weather Service’s Climate Prediction Center (NWS/CPC) along with daily precipitation data from several NWS stations across the southwest were used to characterize the rainfall associated with tropical cyclone remnants as well as total warm season, and annual, rainfall across the region. The areal extent of the TC-associated moisture that was determined from IR and WV imagery was used to extract a TC-remnant-associated precipitation amount. This procedure also sets this work apart from that of Corbosiero et al. (2009) who did not attempt to extract the rainfall associated with only the tropical cyclone they were tracking, but instead acquired the total rainfall from the U.S.-only unified precipitation dataset for the time period of any tropical cyclone they studied. Examples of how tightly coupled our extraction method is to the actual tropical cyclone remnant track can be seen later in this paper (Fig. 5). Station data were also used to quantify the amount of TC-related precipitation at various locations across the southwestern United States.

Several global and regional gridded reanalysis and analysis datasets were used to 1) examine the seasonal variability in the eastern North Pacific and link this to the change in tropical cyclone behavior from the early to the late season, 2) examine the large-scale circulation patterns associated with the individual tropical cyclone remnants, and 3) calculate the composite fields for each group. The 2.5°-resolution 40-yr European Centre for Medium-Range Weather Forecasts (ECMWF) Re-Analysis (ERA-40) product was used for cases prior to 1999, and the Global Forecast System (GFS) final analyses (FNL) at 1° resolution were used for 1999–2005. The 32-km North American Regional Reanalysis (NARR) was used for more detailed analysis of precipitation and other fields over the North American continent (Mesinger et al. 2006). For each candidate tropical cyclone remnant, a grid centered on the tropical cyclone remnant location was extracted from the ERA-40 or FNL analyses every 24 h, and several variables including winds, divergence, vorticity, and geopotential heights, at several different pressure levels (700, 500, and 200 hPa), as well as the mean sea level pressure, were extracted and plotted.

The large-scale circulation patterns, tracks, and rainfall swaths associated with each candidate tropical cyclone

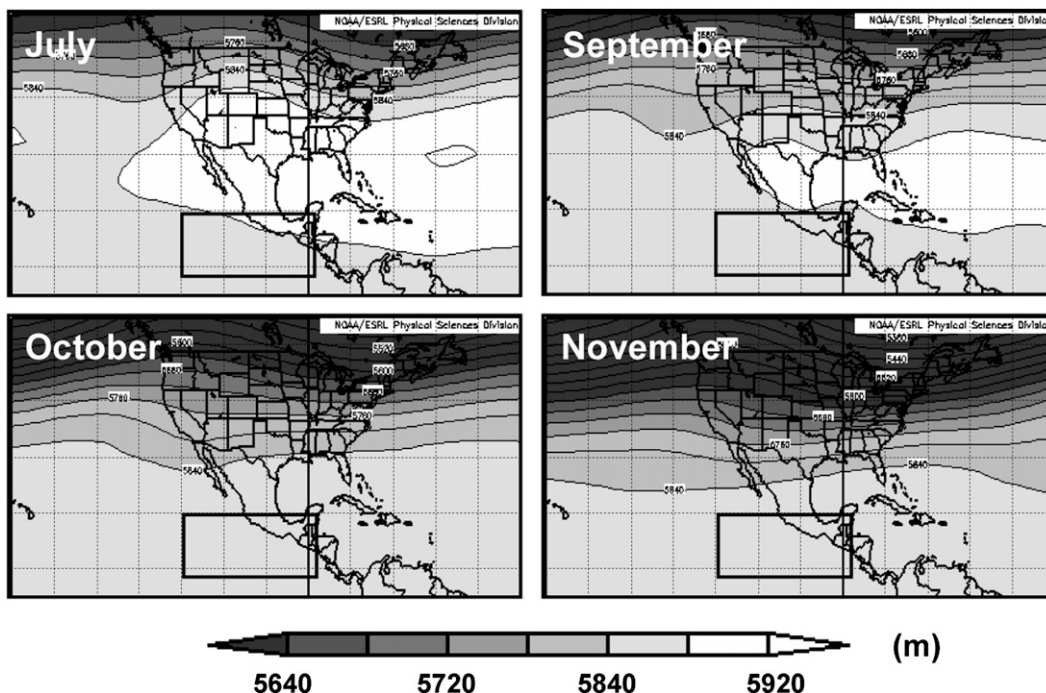


FIG. 1. Mean 500-hPa geopotential height fields (m) averaged over the 1992–2005 study period calculated for July, September, October, and November. Dashed lines indicate 10° latitude–longitude lines. The black box indicates the main genesis region in the eastern North Pacific. Plots made courtesy of the National Oceanic and Atmospheric Administration/Earth System Research Laboratory/Research Physical Sciences Division (NOAA/ESRL/PSD) plotting page online (at <http://www.esrl.noaa.gov/psd/data/composites/day/>).

remnant were examined for common patterns based on 1) whether the track exhibited recurvature to the northeast or straight north-northwest movement, 2) large-scale midlatitude patterns and the nature of the interaction between the tropical cyclone remnants and the midlatitude flow, and 3) whether there was rain associated with the remnant and where it was geographically located. Based on the tracks, rain swaths, and the large-scale patterns, four common categories were identified: two recurving track groups and two straight-moving track groups; in addition, one small group of outliers was also identified.

Composite fields for the four common groups were created by identifying a common time (called the 0-h composite time) in the tropical cyclone track for each group based on the changing characteristics of the tropical cyclone track. For the two recurving track groups the time of recurvature from a westward component to an eastward component to the motion was considered the 0-h composite time. For the two straight-moving tracks, it was the time at which a significant track deflection occurred due to the system approaching the subtropical ridge. Composites at several pressure levels through the atmosphere were then made by averaging the TC-centered geopotential height and wind fields at 48 h prior to the

composite time ($t - 48$ h) through 48 h after the composite time ($t + 48$ h). Note that this method of compositing differs from that of Corbosiero et al. (2009) and allows for a very consistent physical representation of the tropical cyclone remnant relative to the evolving large-scale circulation features.

3. Climatology

a. Seasonal variation of the TC tracks and large-scale flow

Examination of the general circulation pattern of the eastern North Pacific reveals a pattern that is dominated in the tropical regions by the intertropical convergence zone (ITCZ) and a midlatitude regime that is dominated by upper-level troughs. During May–July the region between the equator and 25°N is dominated by weak easterlies, and midlatitude troughs generally remain well to the north (Fig. 1a). During this period, tropical cyclones form in the region between about 8°–18°N and 90°–115°W and propagate in a generally westward direction before dissipating over cooler SSTs (e.g., Lawrence et al. 2001, Fig. 1a). However, as the Northern Hemisphere summer progresses from late summer into autumn, the midlatitude

troughs protrude farther south (Fig. 1). Furthermore, tropical cyclone tracks in the eastern North Pacific tend to shift from westward, to more northwestward later in the season (e.g., Lawrence et al. 2001, Fig. 1b) and interactions between the midlatitude troughs and northward-moving tropical cyclone remnants become more likely. Thus, not only does the chance of interaction with midlatitude troughs increase as the season progresses, but the interactions and subsequent tracks move farther south with the season.

The majority of tropical cyclones that move northward into the midlatitude regime have variable interactions with midlatitude upper-level troughs including, in some cases, a process known as extratropical transition (ET). The ET of tropical cyclones is a common process in many basins with tropical cyclones (e.g., Jones et al. 2003) and is complicated by the nonlinear interactions between the tropical cyclone and midlatitude circulations (e.g., Harr and Elsberry 2000; Hart and Evans 2001; McTaggart-Cowan et al. 2001; Ritchie and Elsberry 2003, 2007). Forecasting the evolution of these systems is extremely difficult over the ocean because accurately predicting the interaction between the tropical cyclone and midlatitude trough is dependent on both the propagation of the trough and the track acceleration as the tropical cyclone moves into the midlatitude westerlies (Ritchie and Elsberry 2007; Kofron et al. 2010a,b). In the eastern North Pacific, very few (less than 10%) of the TCs may begin ET. However, those that do begin ET make rapid landfall in northern Mexico and across the west coast of the United States, complicating the physical processes that occur during ET. The associated precipitation is dependent on both the large-scale dynamics of the trough and tropical cyclone, and on localized orographic effects as the tropical cyclone makes landfall. There are two main issues facing forecasters with regard to these remnant systems: will there be enough moisture advected into the southwestern United States for precipitation to form in the baroclinic environment of a midlatitude trough or will the primary effect be the advection of upper-level cloud cover inhibiting the normal summertime heating that triggers afternoon thunderstorms. We would like to identify patterns associated with particular characteristics of these tropical cyclone remnants as an aid to predicting track and rainfall associated with tropical cyclone remnants that move into the desert southwest region.

b. Eastern North Pacific tropical cyclone rainfall climatology

Figure 2 shows the number of tropical cyclone remnants that crossed into the southwestern United States from the eastern North Pacific by month during the

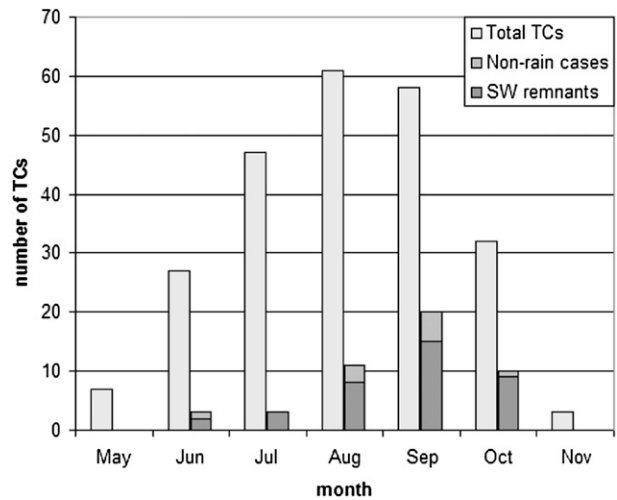


FIG. 2. Histogram of the number of eastern North Pacific TCs during 1992–2005 by month. Included are total numbers, number of TC remnants that brought rainfall to the southwestern United States, and number of TC remnants that did not bring rainfall but had other impacts. Note that the TCs that did not produce rainfall in the United States generally produced rainfall in Mexico.

period 1992–2005. The occurrence of tropical cyclone remnants is skewed to the latter part of the season relative to the total population of eastern North Pacific tropical cyclones. This is related to the tendency for midlatitude upper-level troughs to dig deeper into the tropics later in the season (Fig. 1).

Remnants of 43 tropical cyclones crossed into the southwest region during the 14-yr period of the study. Of these, 35 remnants (81%) brought precipitation to some part of the southwestern United States and the remaining 8 remnants (19%) had precipitation that was almost entirely restricted to Mexico, although cloud cover did advect over the southwestern United States in some of these cases. Thus, on average, 3.1 tropical cyclone remnants impact the southwestern United States each year, accounting for up to 30% of the annual rainfall³ to the region (depending on locality). For example, in 2003 in Tucson, 30% of the annual rainfall fell in just 8 days during two separate tropical cyclone remnant events. The average number of days that were impacted annually by rainfall from remnants was 5.1 at the Tucson International Airport in Arizona and 3.9 at the Albuquerque Sunport in New Mexico.

Figure 3 shows the spatial variation of warm-season precipitation and TC-remnant precipitation as well as

³ Figures are calculated at representative NWS sites for the southwestern United States including the Phoenix International Airport, AZ; the Tucson International Airport, AZ; and the Albuquerque Sunport, NM.

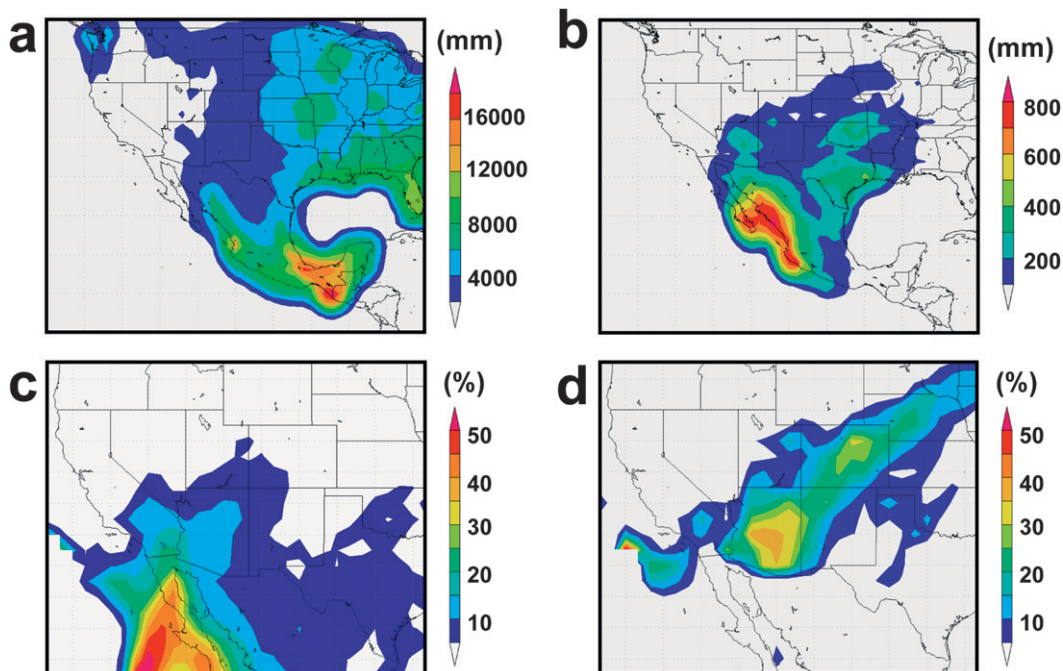


FIG. 3. Areal rainfall over the southwestern U.S. region calculated from the U.S.–Mexico unified gridded precipitation dataset: (a) total warm-season precipitation (15 Jun–31 Oct 1992–2005, mm), (b) total TC precipitation (1992–2005, mm), (c) percentage of warm-season precipitation due to TCs (1992–2005), and (d) percentage of warm-season precipitation due to TCs in 1992.

the percentage of warm-season precipitation that was produced by tropical cyclone remnants over the 14-yr period of the study. For the purposes of this study we have defined the warm season as 15 June–31 October in order to capture the contribution to the rainfall climatology by late-season tropical cyclone remnants. On average, October tropical cyclone remnants impact the region once every approximately 2.5 yr (Table 1). While there is a clear maximum in NAM precipitation over Arizona, New Mexico, and western Texas (Fig. 3a), the TC-contributed rainfall within the United States is maximized in Arizona and western New Mexico, with a second maximum along the Gulf coast of Texas (Fig. 3b). The average contribution of tropical cyclone remnants to the warm-season precipitation (Fig. 3c) appears modest with a maximum in Arizona of 15%–25%. We note that Fig. 3c differs somewhat from a similar figure in Corbosiero et al. (2009), particularly in the coastal precipitation amounts. We speculate that these differences are attributable to 1) the different storm sets studied, 2) the different precipitation datasets used for the analysis, and 3) because we extracted only the TC-related precipitation for our study. However, the inland percentages and general patterns are quite similar. There is considerable annual variability with as much as 50%–60% contribution from TC remnants to the warm-season

precipitation totals in both Arizona and New Mexico in some years (Fig. 3d). There is also substantial variability of the warm season, and annual, precipitation totals both from year to year and within a single year at different geographical locations (Fig. 4a) in the southwestern United States. Although TC remnants can contribute significantly to these warm season totals, there is no correlation with either amount of TC activity (as counted by the number of near-coastal TC remnants) or TC-remnant precipitation totals and anomalously wet or dry years in the region (defined as one standard deviation above or below the 30-yr annual mean). For example, there is almost zero correlation between wetter or drier warm seasons in Tucson and the total amount of TC-related precipitation (Fig. 4). The correlation between total warm-season totals in Tucson and the TC-related precipitation is 0.02.

4. Common large-scale patterns associated with tropical cyclone remnants

The 43 cases of tropical cyclone remnants that crossed into or impacted the southwestern United States in 1992–2005 are examined for characteristic rainfall and large-scale patterns that can be exploited in aiding forecasters. While there is some variability among the cases in terms

TABLE 1. Categories of eastern North Pacific TCs into their common rainfall swath and track types. H = hurricane; TS = tropical storm.

	TC name	Dates
Group 1 (11)	1992 H Darby	6–9 Jul
	1992 H Lester	22–26 Aug
	1993 H Hilary	24–30 Aug
	1994 TS Hector	7–11 Aug
	1998 TS Frank	7–10 Aug
	1999 H Greg	8–13 Sep
	2000 H Carlotta	23–27 Jun
	2001 TS Ivo	13–14 Sep
	2004 TS Blas	13–19 Jul
	2004 H Howard	2–7 Sep
	2004 H Javier	16–21 Sep
Group 2 (8)	1993 H Lidia	11–14 Sep
	1995 H Ismael	13–16 Sep
	1996 H Fausto	12–17 Sep
	1996 H Hernan	3–5 Oct
	1997 TS Olaf/H Pauline	10–14 Oct
	1998 H Madeline	16–20 Oct
	2002 H Kenna	24–28 Oct
	2003 H Nora/H Olaf	6–10 Oct
Group 3 (8)	1993 H Calvin	7–10 Jul
	1997 H Nora	23–26 Sep
	1998 H Isis	2–6 Sep
	1999 H Hilary	20–24 Sep
	2000 H Lane	11–15 Sep
	2001 H Flossie	27 Aug–2 Sep
	2001 H Juliette	23 Sep–4 Oct
	2002 H Hernan	7–8 Sep
Group 4 (8)	1994 H Ileana	12–13 Aug
	1997 TS Carlos	27–28 Jun
	1998 TS Javier	12–15 Sep
	2000 TS Ileana	14–15 Aug
	2000 TS Miriam	16–19 Sep
	2000 TS Norman	22–23 Sep
	2002 TS Genevieve	29 Aug–1 Sep
	2005 H Otis	29 Sep–4 Oct
Group 5 (6)	1994 H Rosa	12–17 Oct
	1995 H Flossie	11–13 Aug
	1997 TS Ignacio	18–20 Aug
	2000 TS Bud	14–19 Jun
	2003 H Ignacio	25–29 Aug
	2003 H Marty	22–26 Sep

of the spatial distribution of rainfall across the southwestern United States, we begin by first broadly dividing the cases into characteristic remnant tracks and rainfall swaths. The topographic forcing that produces spatial variability in the individual tropical cyclone remnant rain swaths is the topic of a future paper. The large-scale patterns associated with the tropical cyclone remnants in each broad category are examined for common features that help explain the shape of the rainfall swath. In particular, the presence and timing or absence of a mid-latitude upper-level trough has a significant impact on the tracks of remnants. Five categories are identified based on the TC-remnant tracks, the large-scale circulation

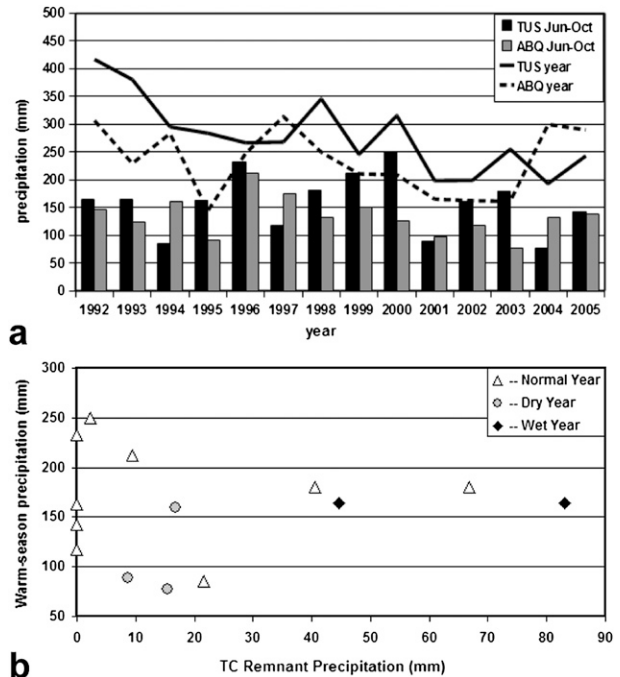


FIG. 4. (a) Histogram of the monsoon and annual rainfall totals for each year from 1992 to 2005 for the NWS sites at the Tucson International Airport and Albuquerque Sunport. (b) Scatterplot of warm-season precipitation recorded at the Tucson NWS site vs TC remnant precipitation (1992–2005). The correlation between the time series is 0.02.

features, and the associated rainfall swaths (Table 1). These groups include group 1, north recurving track (Fig. 5a); group 2, south recurving track (Fig. 5b); group 3, north-northwest movement only (Fig. 5c); group 4, no U.S. rainfall impact (Fig. 5d); and group 5, special cases (not shown).

Composite fields of geopotential heights, vector winds, vorticity, and divergence of the wind at several different pressure levels, and mean sea level pressure, and rainfall for the first four groups are calculated and examined for common features associated with each type of rain swath. The composite fields are a good representation of the individual cases in all four groups with low spatial pattern standard deviations, particularly around the location of the tropical cyclone and between the tropical cyclone and midlatitude flow (Fig. 6). In general, the standard deviations are low prior to the 0-h time and tend to increase subsequent to this (Fig. 6e) with groups 1 and 2, the recurving groups, increasing the most. These results reflect the variability in the structure of the midlatitude flow, the strength of the subtropical ridge, and the size and intensity of the tropical cyclone within each group. However, the relatively low values of standard deviations lend confidence that the composite fields are good representations of the individual members.

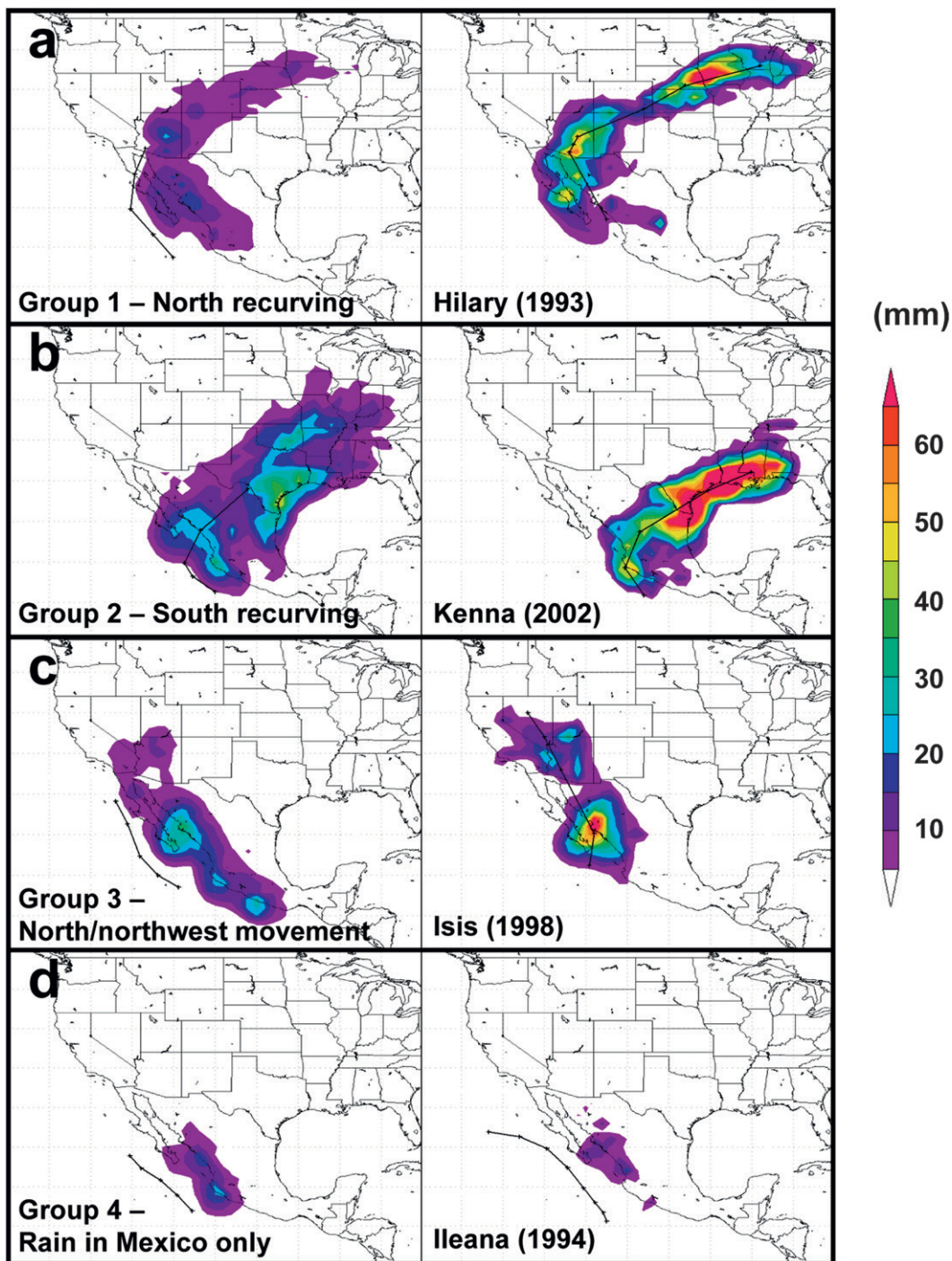


FIG. 5. Average rainfall swath (mm) for groups 1–4 and their representative members. The swaths are created by extracting the rainfall within an area encompassing the moisture transport from a given TC remnant. See Table 1 for the listing of the TCs associated with each group.

a. Group 1: North recurving track

Groups 1 and 2 follow a classic recurvature track due to interaction between the tropical cyclone remnant and a

southward-digging midlatitude trough. Group 1 includes 11 of the 43 cases (Table 1). The cases making up this group generally occur from July to mid-September when midlatitude troughs begin digging south into the tropics

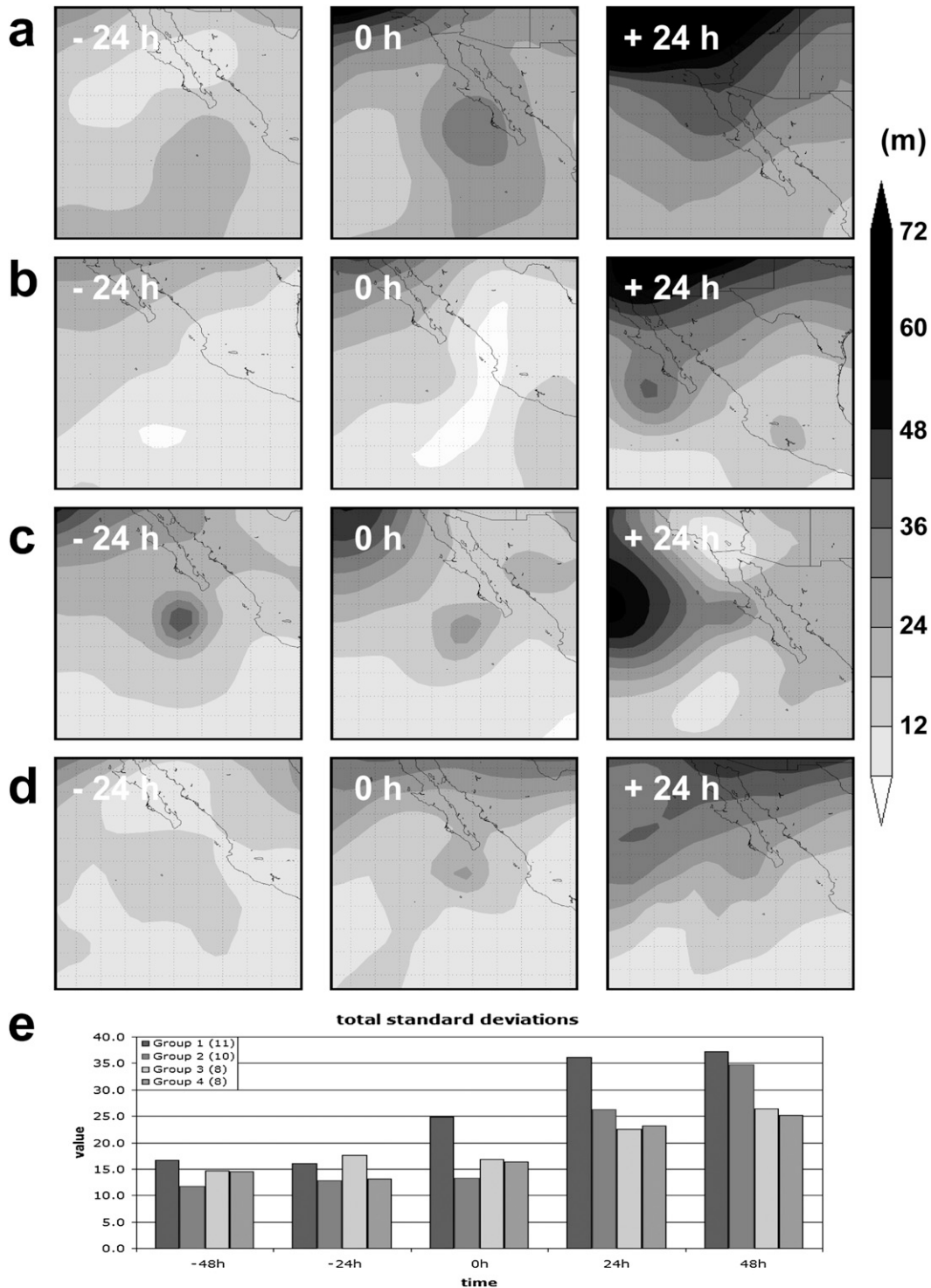


FIG. 6. Standard deviation (m) of the group composite 500-mb geopotential height field at -24 , 0 , and $+24$ h: groups (a) 1, (b) 2, (c) 3, and (d) 4, and (e) time series of the total standard deviations for each group.

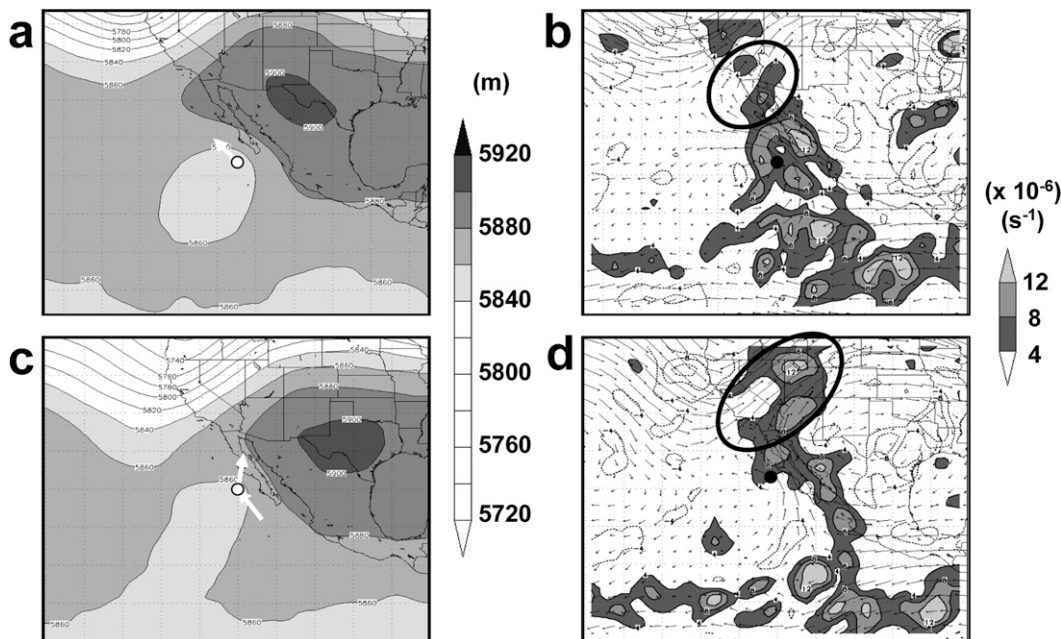


FIG. 7. Group 1 composite fields 24 h prior to the time of recurvature for (a) 500-hPa geopotential height fields (m) and (b) 500-hPa wind vectors (m s^{-1}) and 200-hPa divergence (shaded, $\times 10^{-6} \text{ s}^{-1}$); and at the time of recurvature for (c) 500-hPa geopotential height fields (m) and (d) 500-hPa wind vectors (m s^{-1}) and 200-hPa divergence (shaded, $\times 10^{-6} \text{ s}^{-1}$). The white arrow indicates storm motion.

(Fig. 1b). The more northward location of the group 1 rain swath compared to group 2 is a reflection that, earlier in the season, the low-level steering flow off the Mexico coast steers the tropical cyclones more northward into the midlatitude westerly flow, and the midlatitude troughs that interact with the tropical cyclone remnants to bring them on shore are still relatively far north. The tropical cyclones in group 1 typically recur from northwest to northeast either onshore or just prior to crossing onshore.

The composite rain swath for this group begins on the Baja Peninsula and extends north and northeast into Arizona, New Mexico, Colorado, and northwest Texas before heading east-northeast across the midsection of the United States (Fig. 5a). The remnant track is produced because the tropical cyclone moves northward between a trough to the northwest and the subtropical ridge to the east, interacts with the upper-level midlatitude trough to the northwest (Figs. 7a and 7c), and recurves toward the northeast and east. The early part of the swath is produced as a direct consequence of the tropical cyclone dynamics. As the remnants interact with the trough, the rain swath shifts to the northeast sector (Fig. 5a) where upper-level divergence in the right-rear jet entrance of the trough (Figs. 7b and 7d) and low-level isentropic uplift due to warm air advection by the tropical cyclone circulation (not shown) are the main forcing mechanisms for the precipitation (Ritchie and Elsberry 2007). The remnants

are advected rapidly to the east-northeast under the influence of the midlatitude flow (Figs. 5a, 7a, and 7c) and significant amounts of rainfall continue to fall along the track due to the upper-level support of the trough (Figs. 7b and 7d). The resulting rain swath can extend across much of the continental United States (Fig. 5a) with local rainfall amounts exceeding 60 mm.

The upper-level winds and divergence fields (Figs. 7b and 7d) are typical of an interaction with an upper-level midlatitude trough (e.g., Ritchie and Elsberry 2003, 2007) and are consistent with extratropical transition as documented by Klein et al. (2000) for the western North Pacific. The strongest divergence aloft is associated with the tropical cyclone as it begins to move northward and a secondary maximum is associated with the upper-level trough. As the tropical cyclone moves into the trough, divergence aloft in the right-rear entrance region of the upper-level jet supports vertical motion and the development of precipitation (Jones et al. 2003). The contribution of warm, moist air by the tropical cyclone remnant enhances the rainfall in this region and generally the main rainfall falls to the left of the low-level circulation center track (Klein et al. 2000) (e.g., Fig. 5a).

Group 1 member Hurricane Hilary (1993) follows a pattern similar to that described by the composite fields. Initially, the tropical cyclone moves northward into a weak subtropical ridge (Figs. 8a and 8b). A mobile

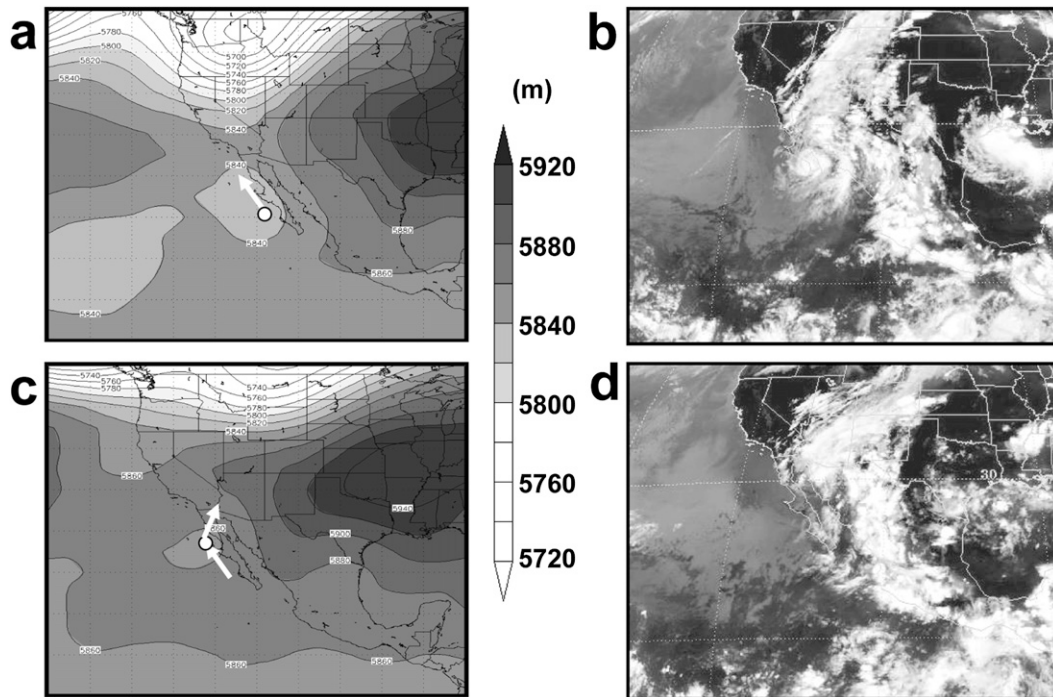


FIG. 8. Group 1 member Hurricane Hilary at 0000 UTC 26 Aug 1993 for (a) 500-hPa geopotential height field (m) and (b) IR satellite image, and at 0000 UTC 27 Aug 1993 for (c) 500-hPa geopotential height field (m) and (d) IR satellite image. The white arrow indicates storm motion.

upper-level trough advects eastward, extending southward into Southern California, and directs a southwesterly flow over the tropical cyclone. The tropical cyclone moves northward through Arizona into the upper-level trough and merges with it in a classic extratropical transition (Figs. 8c and 8d). The resulting rainfall swath extends through central Arizona and then northeastward across the middle part of the country to the northeast (Fig. 5a). As much as 55 mm of rain fell in parts of south-central Arizona during the passage of Hurricane Hilary. Tucson reported 28 mm and Albuquerque reported 45 mm, which is almost 20% of its annual precipitation.

b. Group 2: South recurving track

The more southward location of the group 2 rain swath compared with that of group 1 is a reflection that, later in the season, the low-level steering flow off the Mexico coast steers the tropical cyclones northward into the mid-latitude westerly flow and the midlatitude troughs that interact with the tropical cyclone remnants to bring them on shore have extended as far south as the Baja Peninsula. The composite rainfall swath looks very similar to group 1 and could have been overlaid and included in group 1. However, the composite track lies much farther south geographically, affects different regional forecast centers, and has significant downstream impacts because of the influence of additional moisture from the Gulf of Mexico,

and thus we consider it as a separate group. The “south recurving” group includes 10 of the 43 cases (Table 1), 7 of which occurred in October and the other 3 in mid-September. The tropical cyclones typically recur from northwest to northeast movement prior to crossing on shore and all of the movement over land is toward the northeast.

The composite rain swath for this group begins at the Mexican west coast near (or on the tip of) the Baja Peninsula and extends across Mexico into Texas parallel to the Gulf shore (Fig. 5b). The remnant track is produced because the tropical cyclone moves northward between a southward-digging midlatitude trough to the northwest and a relatively low-amplitude subtropical ridge to the east, interacts with the upper-level trough (Figs. 9a and 9c), and recurves to the northeast. In general, the trough digs farther south than for other groups, extending as far south as the southern tip of the Baja Peninsula. Thus, the remnant tropical cyclone interacts with the midlatitude trough at much lower latitudes compared with group 1. The remnants are advected rapidly to the east-northeast across Mexico and along the Gulf coast (Figs. 5b and 9b) ahead of the trough. A key difference for this group compared with group 1 is that additional moisture is picked up from the Gulf of Mexico, resulting in large amounts of precipitation in all cases. However, the interaction with the midlatitude trough occurs far enough

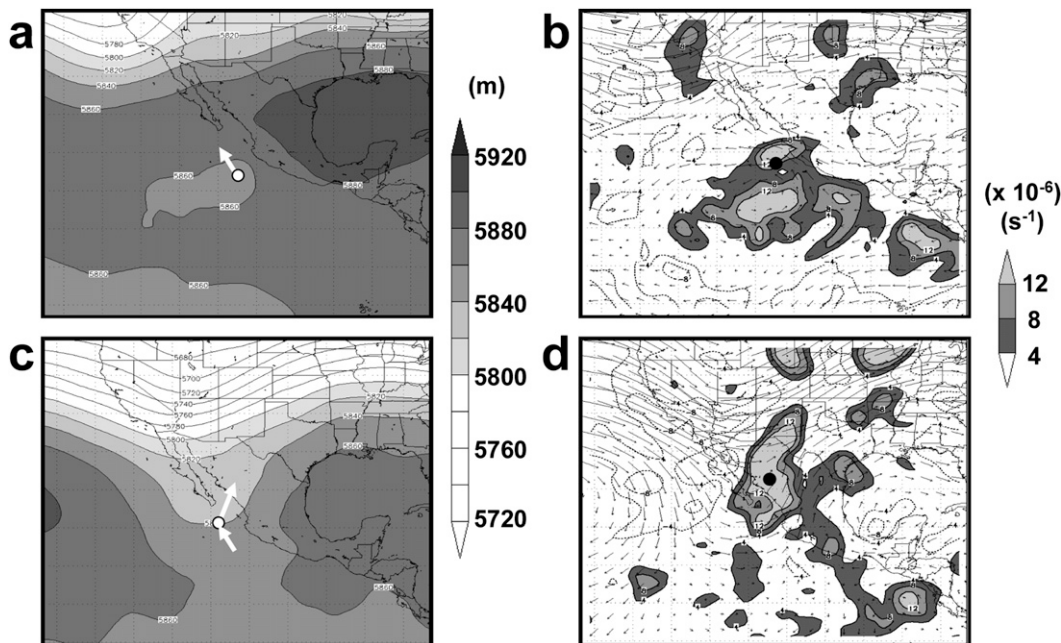


FIG. 9. Group 2 composite fields 24 h prior to the time of recurvature for (a) 500-hPa geopotential height fields (m) and (b) 500-hPa wind vectors (m s^{-1}) and 200-hPa divergence (shaded, $\times 10^{-6} \text{ s}^{-1}$); and 24 h subsequent for (c) 500-hPa geopotential height fields (m) and (d) 500-hPa wind vectors (m s^{-1}) and 200-hPa divergence (shaded, $\times 10^{-6} \text{ s}^{-1}$). The white arrow indicates storm motion.

south to ensure that little precipitation occurs across the southwestern United States.

The upper-level winds and divergence fields are typical of extratropical transition and are qualitatively similar to the group 1 fields. Initially, the strongest upper-level divergence is associated with the tropical cyclone as it begins to move more northward (Fig. 9b). A secondary area of divergence lies in the upper-level trough to the north (Fig. 9b). As the tropical cyclone moves into the trough, divergence aloft in the right-rear entrance region to the upper-level jet supports vertical motion and development of precipitation along and to the left of the low-level track. The contribution of warm, moist air from the Gulf of Mexico enhances the rainfall in this region.

An example of a group 2 tropical cyclone is shown in Figs. 5b and 10. Hurricane Kenna (2002) moved northwest along the western coast of Mexico (Figs. 10a and 10b) until a southward-digging trough picked it up south of the Baja Peninsula (Figs. 10c and 10d). The resulting track moved across Mexico and along the Gulf coast of Texas, picking up additional moisture. Total rainfall amounts exceeded 65 mm along the Gulf coast (Fig. 5b).

c. Group 3: North-northwest movement

The “north and northwest movement only” group includes 8 of the 43 cases (Table 1). It is characterized by

a rain swath that follows the Mexican west coast to the northwest and sometimes turns northward by the time it reaches the United States (Fig. 5c). The composite large-scale pattern is dominated by a ridge in the midlatitudes, well north of the tropical cyclone (Figs. 11a and 11c). A short-wave trough propagates eastward to the north of the tropical cyclone around the centering time of the composite (e.g., Fig. 11a), but has little effect on the tropical cyclone track. The tropical cyclone propagates north and northwest, expanding in size in some cases until it is finally picked up as far north as the Pacific Northwest states by another eastward-moving upper-level trough. The preferred rainfall swath for this category extends northwest along California and Nevada, sometimes extending as far east as western Arizona. Total rainfall amounts tend to be less than for groups 1 and 2.

The upper-level composite winds reflect the gradual drift of the tropical cyclone along the west coast of Mexico and the United States. Maximum upper-level divergence regions remain collocated with the tropical cyclone as it slowly moves north-northwest (Figs. 11b and 11d). A brief region of upper-level divergence moves eastward to the north of the tropical cyclone as a short-wave midlatitude trough advects past at the composite centering time, just far enough away to have little effect on the track of the composite tropical cyclone (not shown). Eventually, by 48 h after the centering time for

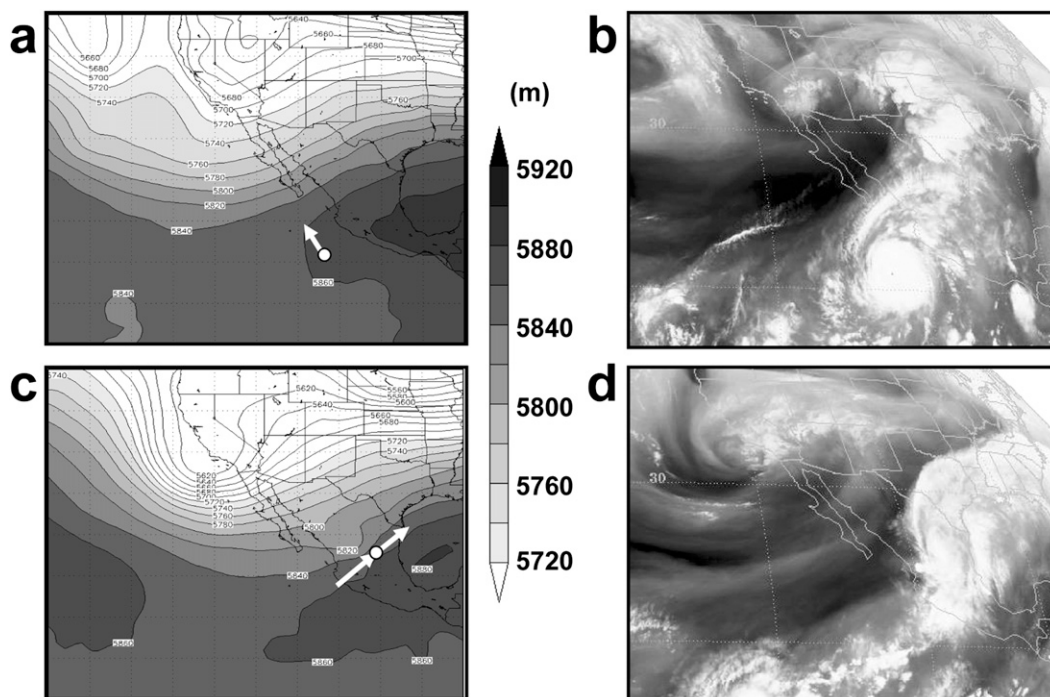


FIG. 10. Group 2 member Hurricane Kenna at 1200 UTC 24 Oct 2002 for (a) 500-hPa geopotential height field (m) and (b) WV satellite image, and at 0000 UTC 26 Oct 2002 for (c) 500-hPa geopotential height field (m) and (d) WV satellite image. The white arrow indicates storm motion.

this group, the composite tropical cyclone is picked up by another midlatitude trough well to the north of the southwestern United States and propagated to the east (not shown).

A typical example of a group 3 tropical cyclone is Hurricane Isis (1998) (Figs. 5c and 12). Hurricane Isis moved gradually north-northwest into a ridge that was located over the western United States (Figs. 12a and 12b). The associated rainfall swath was located over eastern California, western Arizona, and Nevada as the system moved through (Fig. 5c). By the time the remnant of Hurricane Isis had reached the northern Rockies, it was finally picked up by a midlatitude trough propagating onto the continent from the eastern Pacific (e.g., Figs. 12c and 12d).

d. Group 4: No U.S. rainfall

The “no U.S. rainfall” group includes 8 of the 43 cases (Table 1). It is characterized by a rain swath that moves north or northwest along the west coast of Mexico (Fig. 5d). The large-scale pattern is dominated by a westward-building subtropical ridge (Fig. 13), which tends to advect the low-level circulation of the tropical cyclone to the northwest and west. Many individual cases have an approaching midlatitude trough (e.g., Figs. 13a, 13c, 14a, and 14c). However, either the location of the trough is

too far north, or it passes to the north too early, for an interaction with the tropical cyclone circulation to occur. Instead, the upper-level clouds and moisture of the tropical cyclone are frequently advected north and east away from the low-level tropical cyclone circulation and over the southwestern United States (e.g., Fig. 14b). The low-level tropical cyclone circulation finally dissipates over colder sea surface temperatures and the resulting rain swath is limited in extent generally to the Mexican west coast (Fig. 5d).

The upper-level composite winds reflect the gradual drift of the tropical cyclone along the west coast of Mexico as the system slowly weakens. Maximum upper-level divergence regions remain collocated with the tropical cyclone (Figs. 13b and 13d), becoming smaller in areal extent with time. A brief region of upper-level divergence moves eastward well to the north of the tropical cyclone as a midlatitude trough advects past the composite tropical cyclone. As the midlatitude trough passes to the north of the tropical cyclone (Fig. 13d), upper-level outflow from the tropical cyclone is enhanced into the trough, which supports the movement of upper-level clouds from the tropical cyclone over the southwestern United States. However, the trough is too far to the north for a full interaction between the tropical cyclone and trough to occur.

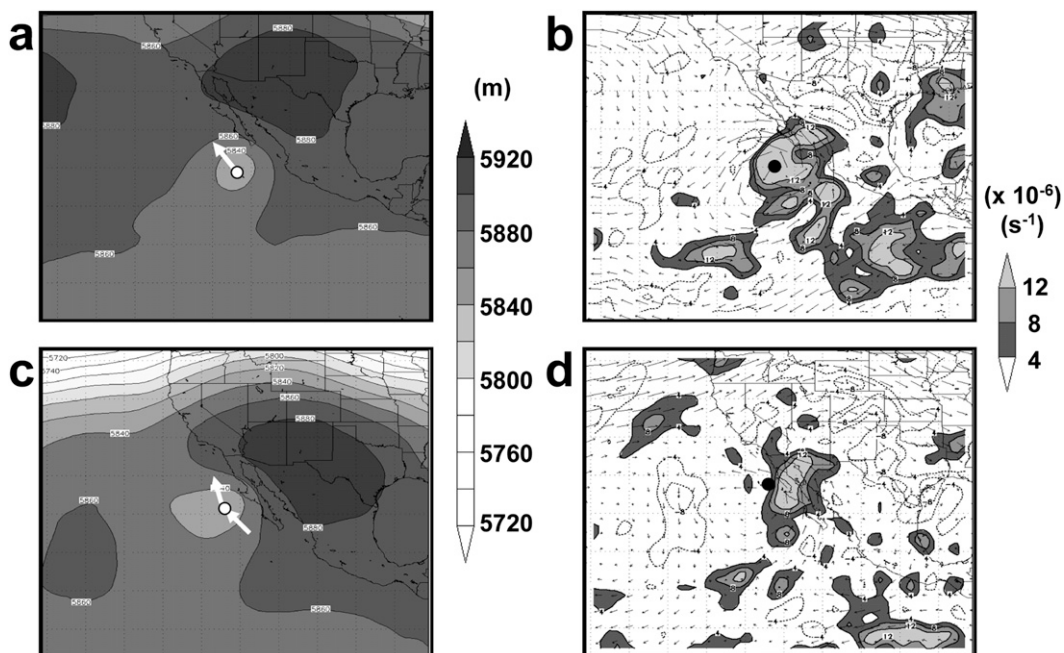


FIG. 11. Group 3 composite fields 24 h prior to the time of recurvature for (a) 500-hPa geopotential height fields (m) and (b) 500-hPa wind vectors (m s^{-1}) and 200-hPa divergence (shaded, $\times 10^{-6} \text{ s}^{-1}$); and 24 h subsequent for (c) 500-hPa geopotential height fields (m) and (d) 500-hPa wind vectors (m s^{-1}) and 200-hPa divergence (shaded, $\times 10^{-6} \text{ s}^{-1}$). The white arrow indicates storm motion.

The most significant impact of the group 4 storms is the potential for advection of high, generally nonprecipitating clouds over the southwestern United States instead of the anticipated tropical cyclone circulation and associated rainfall. The main effect of the clouds is probably to inhibit the normal summertime heating that would typically foster afternoon monsoonal thunderstorms. Thus, rather than being an increased rainfall event, the group 4 tropical cyclone remnants are more likely to be no-rainfall events. The critical aspect of the timing and location of the mid-latitude trough relative to the tropical cyclone remnant circulation and how rapidly the tropical cyclone circulation weakens are all key factors for assessing whether a tropical cyclone remnant will be a group 4 case directly causing little rain to fall or a group 1 or 2 tropical cyclone with some associated rainfall (e.g., Table 2).

An example of a group 4 tropical cyclone is that of Hurricane Ileana (1994) shown in Fig. 14. Hurricane Ileana initially moved parallel to the west coast of Mexico, just offshore. The associated rain swath lies along the coast of Mexico (Fig. 5d). The large-scale pattern consisted of a strong ridge that extended north and west of the tropical cyclone (Fig. 14a) with a mid-latitude trough well to the north. Over the next 24–48 h the subtropical ridge intensified, and the remnants of Hurricane Ileana were steered out to the west by the ridge while the trough passed well to the north of the

tropical cyclone (Fig. 14c). The low-level circulation from Hurricane Ileana continued to move westward and dissipated over colder ocean waters (Fig. 14d).

e. Group 5: Special cases

This category is the catchall for six cases of tropical cyclone remnants from 1992 to 2005 that do not fit into the first four groups. This category contains unusual cases including a tropical cyclone with a diverging rainfall swath affecting two different regions: one tracking to the northeast over New Mexico and Texas similar to a group 1 tropical cyclone and the other moving along the west coast of California into the Pacific Northwest (K. W. Wood and E. A. Ritchie 2010, unpublished manuscript, hereafter WR). The majority of these unusual cases have similarities to the basic four categories, but with enough differences to produce different outcomes from what would otherwise be expected. A future paper documents some of these cases and explores reasons why unusual rain swaths occurred in association with them (WR).

f. Overall characteristics for forecasting

While general forecasting for these remnants relies considerably on the skill of numerical weather prediction models, some overall characteristics that may help decision making regarding these extremely difficult events

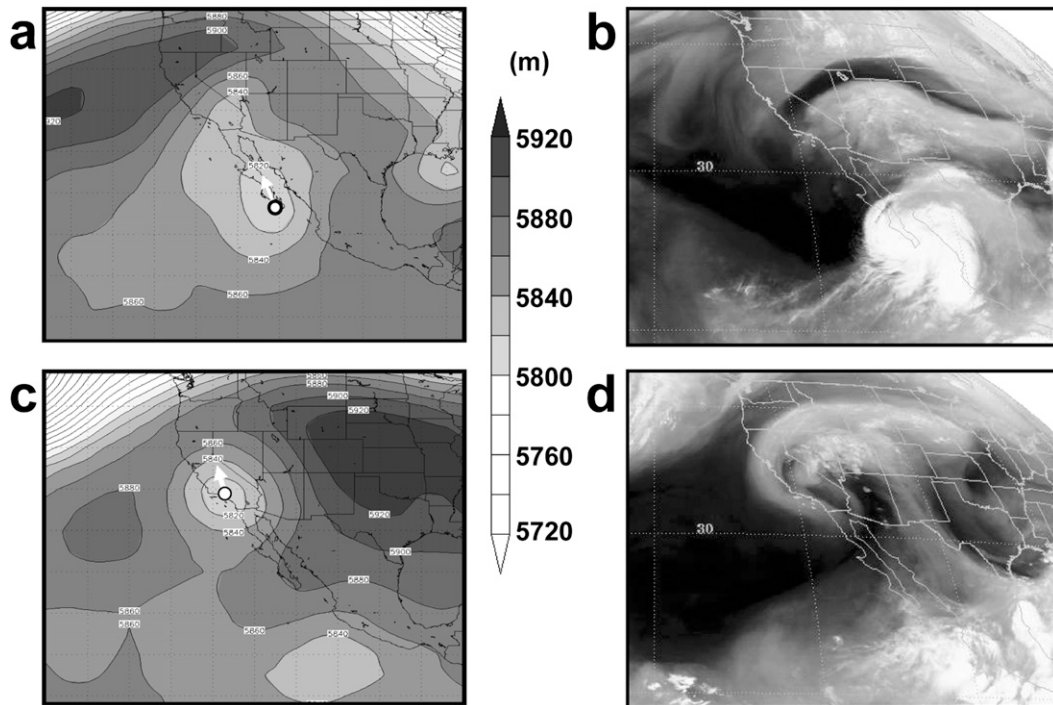


FIG. 12. Group 3 member Hurricane Isis at 1200 UTC 2 Sep 1998 for (a) 500-hPa geopotential height field (m) and (b) WV satellite image, and at 1200 UTC 5 Sep 1998 for (c) 500-hPa geopotential height field (m) and (d) WV satellite image. The white arrow indicates storm motion.

are summarized in Table 2. The categories can be divided into two broad categories: those that recurve to the east over the United States and those that do not. Those that recurve to the east are usually tropical cyclone remnants that interact with, and become absorbed into, a midlatitude trough or cut-off low that carries the remnant moisture over the United States. They divide into two distinct categories based on the latitude at which the interaction and subsequent rainfall swath occurs. Group 1 remnants tend to recurve at a more northern location than group 2 remnants. This is because they occur earlier in the season (late June–early September) when the baroclinic zone and midlatitude troughs are farther north (Figs. 1a and 1b). For these cases the average latitudinal location of the 500-hPa 5840-m contour (chosen because it best represents the base of the mean midlatitude troughs at 500 hPa in the summertime) in the baroclinic zone is located at approximately 38°N and the average latitude location of the tropical cyclone at the time of recurvature is 25°N (Table 2). In contrast, the group 2 cases occur in mid-September–October, for which the average latitudinal location of the 500-hPa 5840-m contour in the baroclinic zone is located at approximately 31°N and the average latitude location of the tropical cyclone at the time of recurvature is 20°N (Table 2). The groups vary longitudinally as well with group 1 tropical cyclones recurving

115°W on average compared with 109°W for group 2 cases. These values are statistically significant differences using a two-sample, equal-variance Student's t test at the 1% level, and it clearly suggests that there is a good differentiation between the locations of the two remnant populations.

The geographic differences between the group 1 and 2 remnants are important because the more southward location of the group 2 average track results in a reduced impact in the southwestern United States and an influx of additional moisture from the Gulf of Mexico being entrained into the synoptic environment as the remnants track along the Gulf coast. Group 2 rainfall swath maximum amounts exceed 65 mm in almost all cases whereas group 1 maximum rainfall averaged approximately 28 mm.

The primary considerations for whether a remnant will be a group 1 or 2 case or whether it be a group 3 or 4 case appear to be

- 1) the distance between the remnant and any midlatitude trough/cut-off low needs to be within approximately 9° latitude of the edge of the trough at recurvature time (e.g., Figs. 15a and 15b),
- 2) the trough/cut-off low should be to the northwest of the remnant at recurvature time, and

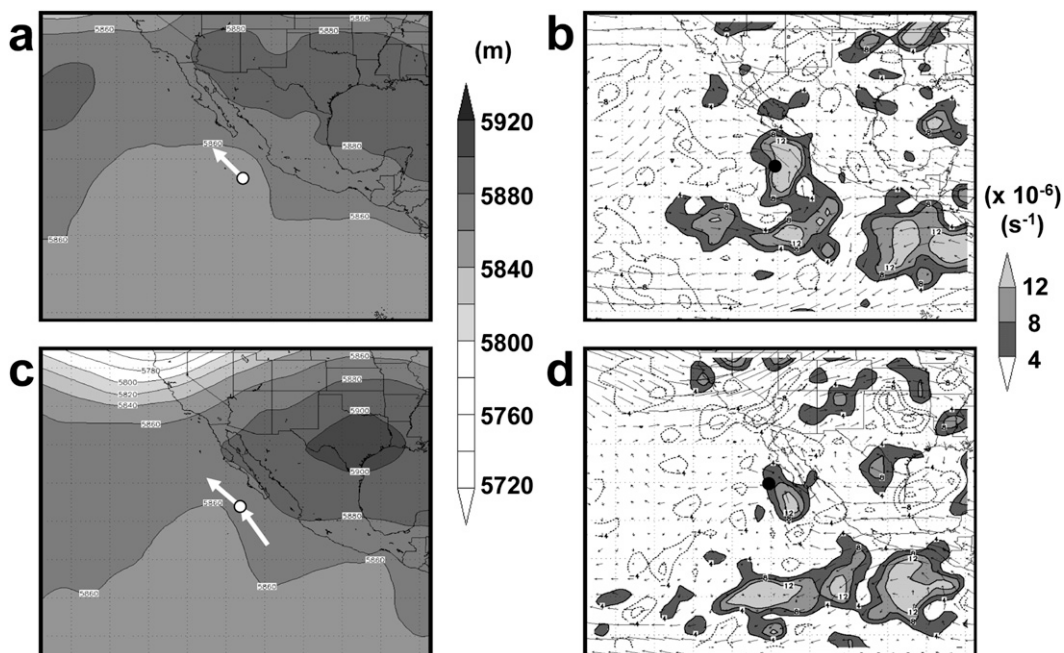


FIG. 13. Group 4 composite fields 24 h prior to closest approach to the ridge for (a) 500-hPa geopotential height fields (m) and (b) 500-hPa wind vectors (m s^{-1}) and 200-hPa divergence (shaded, $\times 10^{-6} \text{ s}^{-1}$); and 24 h subsequent for (c) 500-hPa geopotential height fields (m) and (d) 500-hPa wind vectors (m s^{-1}) and 200-hPa divergence (shaded, $\times 10^{-6} \text{ s}^{-1}$). The white arrow indicates storm motion.

- 3) the ridge between the trough and the remnant should be weak (10–20-m amplitude change; Fig. 15a) or nonexistent (Fig. 15b).

The primary difference between groups 1 and 2 is the latitudinal location of the baroclinic zone (and thus the midlatitude trough) and the resulting rainfall impacts on the southwestern United States.

Groups 3 and 4 remnants do not recurve to the east over the United States, at least not until they have moved very far north, well beyond the boundaries of the southwest region. Group 3 remnants can bring rainfall to the west coast of the United States (Fig. 5c) and group 4 remnants typically bring rainfall to only the west coast of Mexico but may bring cloud cover and cooler temperatures over parts of the southwestern United States. The primary considerations for these two groups are that the baroclinic zone is located up to 16° latitude farther north than the tropical cyclone remnant compared with approximately 9° latitude for groups 1 and 2 (Table 2). The flow is much more zonal with low-amplitude troughs in the baroclinic zone and the subtropical ridge located between the tropical cyclone remnant and any possible midlatitude low pressure system has a higher relative amplitude of 40 m compared with 10–20 m for groups 1 and 2. The main consequence of this separation from the midlatitude regime is that the large-scale steering over

the tropical cyclone remnants is to the northwest and west. Separating group 3 from group 4 remnants based on the statistical quantities in Table 2 is problematic. The statistical quantities are very similar for both categories.

5. Discussion and summary

Forty-three eastern North Pacific tropical cyclone remnants that affected the southwestern United States during 1992–2005 were investigated. On average 3.1 remnants impacted the region annually during the 14-yr period. Out of 43 cases, 35 brought rainfall to the southwestern United States and some of the remaining 8 brought cloud cover, which impacted the normal summertime afternoon thunderstorm pattern.

The cases were investigated for common large-scale circulation and rainfall patterns. Four main patterns were identified: north recurving track (25%), south recurving track (23%), north-northwest movement only (19%), and no U.S. rainfall (19%). Six of the tropical cyclone cases currently are not included in these categories (14%). The rainfall swaths for each tropical cyclone remnant case were extracted from the 1° latitude–longitude U.S.–Mexico unified precipitation dataset. The remnant tracks and rainfall swaths were modulated by particular large-scale circulation patterns, which made it

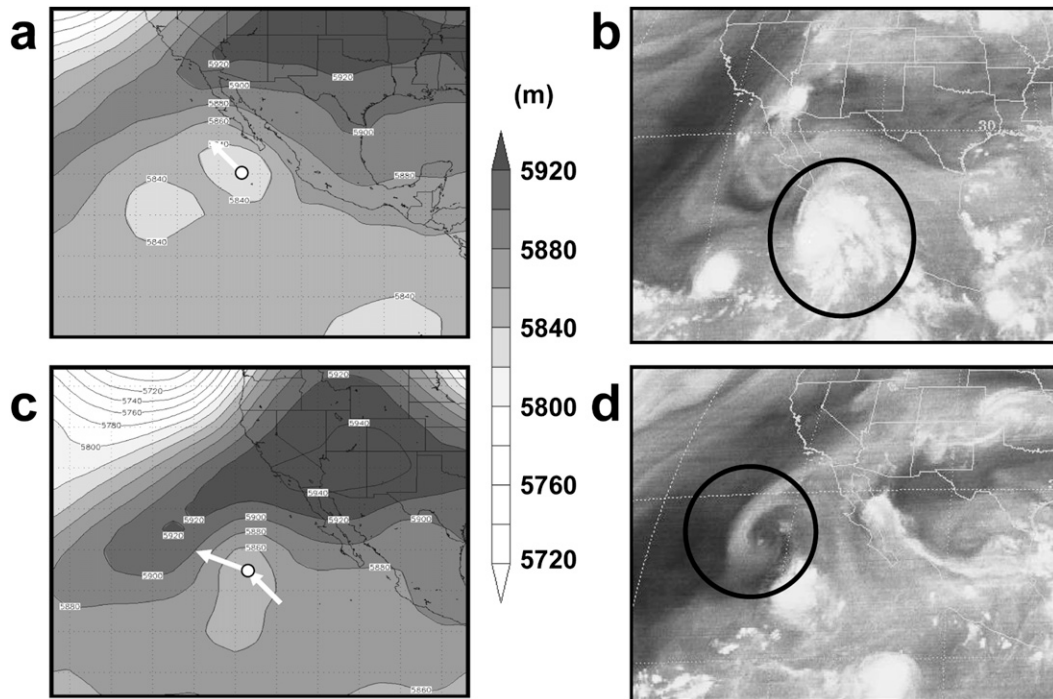


FIG. 14. Group 4 member Hurricane Ileana at 1200 UTC 12 Aug 1994 for (a) 500-hPa geopotential height field (m) (b) WV satellite image, and at 1200 UTC 14 Aug 1994 for (c) 500-hPa geopotential height field (m) and (d) WV satellite image. The black ellipses in (b) and (d) highlight the remnants of Ileana at each time. The white arrow indicates storm motion.

possible to characterize the flows associated with each expected rainfall swath. There can be considerable variability in the rainfall amounts at different locations along each swath, due in part, to differences in topography. However, using some simple rules based on the composite patterns, the gross characteristics of the rainfall swath—its extent and track—can be ascertained based on the

expected timing and interaction between the large-scale circulation and the tropical cyclone remnants.

Future work will include increasing and updating the dataset. Currently, 1989–91 and 2006–09 are being added. In addition, we would like to improve on our more subjective characterization of the large-scale flow and rainfall patterns using objective statistical methods to more

TABLE 2. General characteristics of the large-sale circulation and TCs for each group.

Characteristics	Group 1	Group 2	Group 3	Group 4
Presence of trough	Important—ET scenario	Important—ET scenario	Not important	Not important
Presence of ridge	Weak/broken	Weak/broken	Unbroken/building to west	Unbroken/building to west
Time of season	Early season: Jul–early Sep	Late season: mid-Sep–Oct	Jul–Sep	Jun–Oct
Distance from TC to trough at recurvature	<10° lat ($\sigma = 2.8^\circ$)	<10° lat ($\sigma = 4.6^\circ$)	>15° lat (avg: 18°) ($\sigma = 4.9^\circ$)	>15° lat (avg: 17°) ($\sigma = 4.9^\circ$)
Location of midlatitude trough	To the northwest of TC remnant	To the northwest of TC remnant	N/A	N/A
Mean lat of the 5840-m contour (°N)	37.5	31	38	37
Mean TC lat (°N)	25 ($\sigma = 3.1^\circ$)	20 ($\sigma = 2.3^\circ$)	22 ($\sigma = 3.4^\circ$)	21 ($\sigma = 2.3^\circ$)
Mean TC lon (°W)	115 ($\sigma = 4.9^\circ$)	109 ($\sigma = 2.8^\circ$)	113 ($\sigma = 4.1^\circ$)	112 ($\sigma = 5.2^\circ$)
Δ lat for 5840-m contour and TC	7°	8°	13°	12°

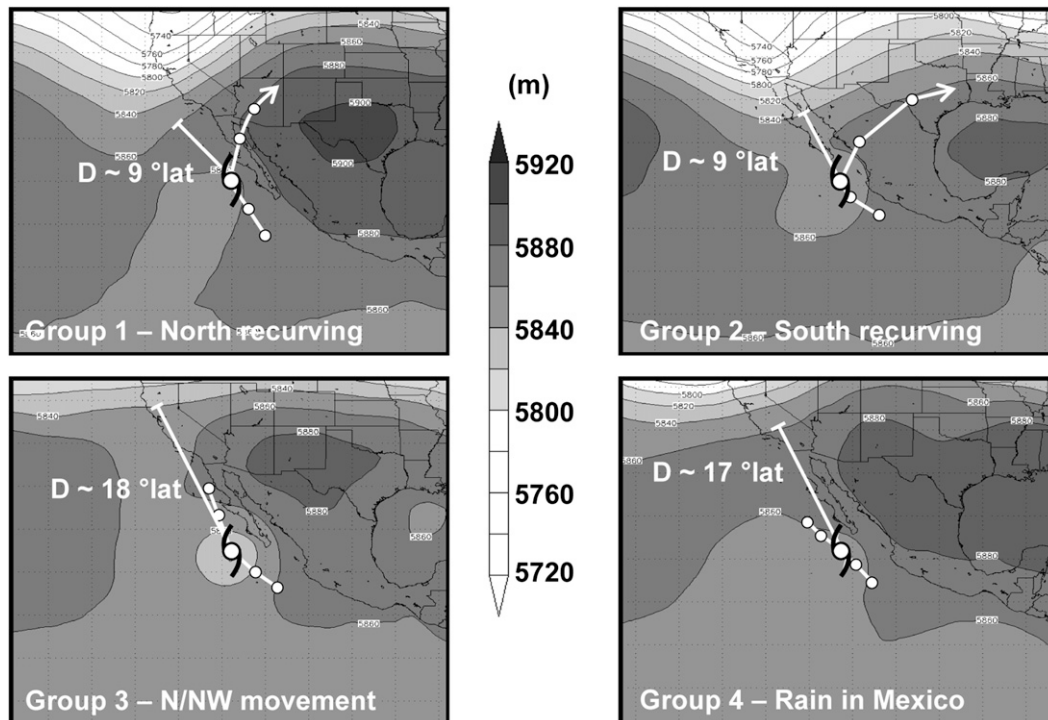


FIG. 15. Composite plots of 500-hPa geopotential height fields (m) for the four categories at 0 h showing the orientation and distance of the TC to the nearest point in the midlatitude trough. The white arrow indicates storm motion.

robustly separate the patterns. A final task is to run a series of simulations forced by the observed large-scale flows in order to characterize the detailed rainfall patterns due to topography along each rainfall swath.

Acknowledgments. Some of the figures presented here were produced using the NOAA Earth System Research Laboratory Research Physical Sciences Division reanalysis plotting page. The manuscript has been improved by the comments of two anonymous reviewers. This study has been supported, in part, by the National Oceanic and Atmospheric Administration (NOAA) under Grant NA030AR4310085 and by a State of Arizona Technology Research Initiative Fund-Water Sustainability Program grant.

REFERENCES

Adams, D. K., and A. C. Comrie, 1997: The North American monsoon. *Bull. Amer. Meteor. Soc.*, **78**, 2197–2213.
 Bieda, S. W., C. L. Castro, S. L. Mullen, A. C. Comrie, and E. Pytlak, 2009: The relationship of transient upper-level troughs to variability of the North American monsoon system. *J. Climate*, **22**, 4213–4227.
 Collins, J. M., and I. M. Mason, 2000: Local environmental conditions related to seasonal tropical cyclone activity in the northeast Pacific basin. *Geophys. Res. Lett.*, **27**, 3881–3884.

Comrie, A. C., and E. C. Glenn, 1998: Principal components-based regionalization of precipitation regimes across the southwest United States and northern Mexico, with an application to monsoon precipitation variability. *Climate Res.*, **10**, 201–215.
 Corbosiero, K. L., M. J. Dickinson, and L. F. Bosart, 2009: The contribution of eastern North Pacific tropical cyclones to the rainfall climatology of the southwest United States. *Mon. Wea. Rev.*, **137**, 2415–2435.
 Douglas, A. V., and P. J. Englehart, 2007: A climatological perspective of transient synoptic features during NAME 2004. *J. Climate*, **20**, 1947–1954.
 Douglas, M. W., and J. C. Leal, 2003: Summertime surges over the Gulf of California: Aspects of their climatology, mean structure, and evolution from radiosonde, NCEP reanalysis, and rainfall data. *Wea. Forecasting*, **18**, 55–74.
 —, R. A. Maddox, K. Howard, and S. Reyes, 1993: The Mexican monsoon. *J. Climate*, **6**, 1665–1677.
 Englehart, P. J., and A. V. Douglas, 2001: The role of eastern North Pacific tropical storms in the rainfall climatology of western Mexico. *Int. J. Climatol.*, **21**, 1357–1370.
 —, and —, 2006: Defining intraseasonal rainfall variability within the North American monsoon. *J. Climate*, **19**, 4243–4253.
 Etheredge, D., D. S. Gutzler, and F. J. Pazzaglia, 2004: Geomorphic response to seasonal variations in rainfall in southwest North America. *Geol. Soc. Amer. Bull.*, **116**, 606–618.
 Finch, Z. O., and R. H. Johnson, 2010: Observational analysis of an upper-level inverted trough during the 2004 North American Monsoon Experiment. *Mon. Wea. Rev.*, **138**, 3540–3555.
 Fuller, R. D., and D. J. Stensrud, 2000: The relationship between tropical easterly waves and surges over the Gulf of California

- during the North American monsoon. *Mon. Wea. Rev.*, **128**, 2983–2989.
- Gutzler, D. S., 2004: An index of interannual precipitation variability in the core of the North American monsoon region. *J. Climate*, **17**, 4473–4480.
- , and Coauthors, 2005: The North American Monsoon Model Assessment Project (NAMAP): Integrating numerical modeling into a field-based process study. *Bull. Amer. Meteor. Soc.*, **86**, 1423–1429.
- , and —, 2009: Simulations of the 2004 North American monsoon: NAMAP2. *J. Climate*, **22**, 6716–6740.
- Harr, P. A., and R. L. Elsberry, 2000: Extratropical transition of tropical cyclones over the western North Pacific. Part I: Evolution of structural characteristics during the transition process. *Mon. Wea. Rev.*, **128**, 2613–2633.
- Hart, R. E., and J. L. Evans, 2001: A climatology of the extratropical transition of Atlantic tropical cyclones. *J. Climate*, **14**, 546–564.
- Higgins, R. W., and W. Shi, 2005: Relationships between Gulf of California moisture surges and tropical cyclones in the eastern Pacific basin. *J. Climate*, **18**, 4601–4620.
- , Y. Yao, and X. L. Wang, 1997: Influence of the North American monsoon system on the U.S. summer precipitation regime. *J. Climate*, **10**, 2600–2622.
- , Y. Chen, and A. V. Douglas, 1999: Interannual variability of the North American warm season precipitation regime. *J. Climate*, **12**, 653–680.
- , W. Shi, and C. Hain, 2004: Relationships between Gulf of California moisture surges and precipitation in the southwestern United States. *J. Climate*, **17**, 2983–2997.
- Jáuregui, E., 2003: Climatology of landfalling hurricanes and tropical storms in Mexico. *Atmósfera*, **16**, 193–204.
- Jones, S., and Coauthors, 2003: The extratropical transition of tropical cyclones: Forecast challenges, current understanding, and future directions. *Wea. Forecasting*, **18**, 1052–1092.
- Klein, P. M., P. A. Harr, and R. L. Elsberry, 2000: Extratropical transition of western North Pacific tropical cyclones: An overview and conceptual model of the transformation stage. *Wea. Forecasting*, **15**, 373–395.
- Kofron, D. E., E. A. Ritchie, and J. S. Tyo, 2010a: Determination of a consistent time for the extratropical transition of tropical cyclones. Part I: Examination of existing methods for finding “ET time.” *Mon. Wea. Rev.*, **138**, 4328–4343.
- , —, and —, 2010b: Determination of a consistent time for the extratropical transition of tropical cyclones Part II: Potential vorticity metrics. *Mon. Wea. Rev.*, **138**, 4344–4361.
- Larson, J., Y. Zhou, and R. W. Higgins, 2005: Characteristics of landfalling tropical cyclones in the United States and Mexico: Climatology and interannual variability. *J. Climate*, **18**, 1247–1262.
- Lawrence, M. B., L. A. Avila, J. L. Beven, J. L. Franklin, R. J. Pasch, and S. R. Stewart, 2001: Eastern North Pacific hurricane season of 2000. *Mon. Wea. Rev.*, **129**, 3004–3014.
- McTaggart-Cowan, R., J. R. Gyakum, and M. K. Yau, 2001: Sensitivity testing of extratropical transitions using potential vorticity inversions to modify initial conditions: Hurricane Earl (1998) case study. *Mon. Wea. Rev.*, **129**, 1617–1636.
- Mesinger, F., and Coauthors, 2006: North American Regional Reanalysis. *Bull. Amer. Meteor. Soc.*, **87**, 343–360.
- Reyes, S., and A. Mejía-Trejo, 1991: Tropical perturbations in the eastern Pacific and the precipitation field over north-western Mexico in relation to the ENSO phenomenon. *Int. J. Climatol.*, **11**, 515–528.
- Ritchie, E. A., and R. L. Elsberry, 2003: Simulations of the extratropical transition of tropical cyclones: Contributions by the midlatitude upper-level trough to reintensification. *Mon. Wea. Rev.*, **131**, 2122–2128.
- , and —, 2007: Simulations of the extratropical transition of tropical cyclones: Phasing between the upper-level trough and tropical cyclone. *Mon. Wea. Rev.*, **135**, 862–876.
- , D. Szenasi, and D. S. Gutzler, 2006: The impact of tropical cyclone remnants on the rainfall of the North American southwest region. Preprints, *27th Conf. on Hurricanes and Tropical Meteorology*, Monterey, CA, Amer. Meteor. Soc., 13D.4 [Available online at <http://ams.confex.com/ams/pdfpapers/137924.pdf>.]
- Stensrud, D. J., R. L. Gall, and M. K. Nordquist, 1997: Surges over the Gulf of California during the Mexican monsoon. *Mon. Wea. Rev.*, **125**, 417–437.